General Disclaimer

One or more of the Following Statements may affect this Document

JPL PUBLICATION 78-3

A Study of Forecast Growth with a Barotropic Model of the Atmosphere

(NASA-CR-156138) A STUDY OF FORECAST GROWTH WITH A BARCTFCPIC MODEI OF THE ATMCSPHERE (Jet Propulsion Lab.) 30 p HC A03/MF A01 CSCL 04E

N78-20718

Unclas
G3/47 11864

National Aeronautics and
Space Administration

Jet Propulsion Laboratory
California Institute of Technology
Pasadena, California 91103

TECHNICAL REPORT STANDARD TITLE PAGE

1. Report No. JPL Pub. 78-3	2. Government Accession No.	3. Recipient's Catalog No.
4. Title and Subtitle A Study of Forecast Growth with a Barotropic Model of the Atmosphere		5. Report Date April 1, 1978
		6. Performing Organization Code
7. Author(s) Isidoro M. Halberstam		8. Performing Organization Report No.
9. Performing Organization Name and Address JET PROPULSION LABORATORY California Institute of Technology 4800 Oak Grove Drive Pasadena, California 91103		10. Work Unit No.
		11. Contract or Grant No. NAS 7-100
		13. Type of Report and Period Covered JPL Publication
12. Sponsoring Agency Name and Address NATIONAL AERONAUTICS AND SPACE ADMINISTRATION Washington, D.C. 20546		14. Sponsoring Agency Code

15. Supplementary Notes

16. Abstract

A barotropic model of the atmosphere is used to text various sources of forecast error. These errors are classified as truncation error, physical error, or initial error. It is shown that growth patterns due to each category differ significantly. Initial errors are shown not to grow in a barotropic model contrary to reports of other studies which indicate that they basically do grow. Also, random initial errors are shown to decrease due to the filtering effect of the model itself. Results seem to indicate that instabilities are required for error growth, be they barotropic or baroclinic, and that random errors are not representative of true initial conditions.

17. Key Words (Selected by Author(s)) Meteorology and Climatology	18. Distribution Statement Unclassified - Unlimited

19. Security Classif. (of this report)	20. Security Classif. (of this page)	21. No. of Pages	22. Price
Unclassified	Unclassified	32	

JPL PUBLICATION 78-3

A Study of Forecast Growth with a Barotropic Model of the Atmosphere

Isidore M. Halberstam

April 1, 1978

National Aeronautics and
Space Administration

Jet Propulsion Laboratory
California Institute of Technology
Pasadena, California 91103

Preface

The work described in this report was performed by the Earth and Space Sciences Division of the Jet Propulsion Laboratory.

Acknowledgement

This report presents the results of one phase of research carried out by the Jet Propulsion Laboratory, California Institute of Technology, under contract NAS-7-100, sponsored by the Seasat Program Office, Office of Applications, National Aeronautics and Space Administration.

Contents

Abstract

A barotropic model of the atmosphere is used to test various sources of forecast error. These errors are classified as truncation error, physical error, or initial error. It is shown that growth patterns due to each category differ significantly. Initial errors are shown not to grow in a barotropic model contrary to reports of other studies which indicate that they basically do grow. Also, random initial errors are shown to decrease due to the filtering effect of the model itself. Results seem to indicate that instabilities are required for error growth, be they barotropic or baroclinic, and that random errors are not representative of true initial conditions.

I. INTRODUCTION

With the launching of Seasat in Spring, 1978, a significant amount of meteorological data will be added to the forecasters inventory. Two of the satellite's sensors will provide much needed information on the oceans' surface temperature and wind stress. These may be incorporated into the initial data sets of large numerical forecasting models and hopefully reduce errors in forecasting. Before estimates can be made, however, on the effectiveness of these new data, or of any satellite observations, for that matter, it is necessary to understand the nature of forecasting errors, in general, and the role increased observations can play in reducing them.

Errors in weather forecasts are generally broken down into three main categories:

1. Physical error due to poor representation of the actual phenomena by the mathematical equations.
2. Truncation error due to finite difference approximation of the governing equations, and
3. Initialization error due to inaccurate portrayal of the initial conditions.

The physical error is generally due to a lack of knowledge concerning the physical processes of the atmosphere, or, because of computer limitations, certain phenomena are compromized with coarse parameterizations. That is to say, that processes, such as radiation, for example, may require frequent calculation of small components such as absorption by wavelength bands, but, because of time limitations, the wavelengths are broken into only 3 or 4 bands and the absorption and transmission at these bands treated with some simple, bulk coefficients. Because these parameterizations are, by definition, only approximations to the true case, one would expect some error to result from their use. How great this error may become can only be approximated by simulations where more precise equations are used for a limited time. In processes where no exact mathematical representation is known, no real assessment of the physical error can be furnished.

Truncation errors are a general category embodying all errors that may result from the use of a coarse grid for a finite difference solution to the governing equations. In a mathematical sense, the errors are due solely to the use of finite-differences instead of exact derivatives. From a physical perspective, the use of a coarse grid filters many of the small scale phenomena which may still be important to weather forecasting. Miyakoda, et al., (1971) have demonstrated the effects of increasing model resolution by forecasting with several versions of the Geophysical Fluid Dynamics Laboratory (GFDL) 9-level general circulation model (GCM). There are significant impacts on the forecast when the grid spacing is decreased from 540 to 270 km but much smaller impacts when it is further decreased to 135 km. Apparently the processes which are omitted in the very coarse grid are quite important even for short-range forecasts, while there is little contribution to the short-range forecasts from the smaller scale. The 135 km-grid did become significant after about 5 to 6 days, however, proving that even small scale phenomena are important for longer range forecasts.

Initial errors include all deviations of the model's initial state from the true initial state. These deviations can be caused by random instrument error, human error, omission of large areas, and the subsequent interpolation errors involved in applying the sparse observations to the grid points. These various sources may not all result in the same type of error distribution. In fact, the random instrument error is generally of low magnitude and independent of location. The other errors (excluding human error) are geographically dependent, with the oceans and uninhabited areas notoriously lacking in meteorological observations.

In practice, it is difficult to separate the influences of these individual error sources, although attempts have been made to simulate the various error patterns associated with each. Much of the concern over error growth has been stimulated by the necessity to incorporate satellite data into numerical models of the atmosphere; Kasahara (1972) presents a summary of various studies on the nature of data assimilation into numerical models and briefly reviews the progress in understanding initial error growth. Bengtsson (1975), too, discusses the nature of errors in relation to the assimilation of satellite data into numerical models of the atmosphere as does Blumen (1976a) and Blumen (1976b). The work here intends to compare the various sources of error and their effects on a simplified, non-linear model of the atmosphere. Understanding these various errors will help in the assessment of impacts on forecasts due to the assimilation of current and projected satellite data. Part of this study was assimilated into the Seasat simulation experiments conducted at the Goddard Institute for Space Studies (GISS) and described by Cane, et al. (1977).

II. DESCRIPTION OF THE EXPERIMENT

The model selected for studies of error growth was the simple, shallow water equations, which assumes a barotropic, inviscid, incompressible fluid with height-independent velocities. These equations have been used for assimilation studies, in either their primitive form or in their differentiated vorticity form, by many researchers including Blumen (1976a), Morel, et al., (1971), and Miyakoda and Talagrand (1971), and Halberstam (1974). The governing equations are:

(1) a. $\partial u/\partial t + u\, \partial u/\partial x + v\, \partial u/\partial y = -g\, \partial h/\partial x - fv$

b. $\partial v/\partial t + u\, \partial v/\partial x + v\, \partial v/\partial y = -g\, \partial h/\partial y + fu$

c. $\partial h/\partial t + u\, \partial h/\partial x + v\, \partial h/\partial y = -h\, (\partial u/\partial x + \partial v/\partial y)$,

where u and v are the westerly and southerly wind components, h is the height of the fluid, f is a coriolis parameter, and g is earth's (constant) gravitational acceleration. The boundaries were cyclical in the x-direction and impenetrable, yet frictionless at y=0 and y=Y. f was assumed equal to $2\Omega = 7.2 \times 10^{-4}$ s.$^{-1}$. The latitudinal variation in the model was from 20N to 70N.

Most runs were made with a resolution of about 2-1/2° in the meridional direction and about 5° of longitude in the latitudinal direction. This employed a grid system of 42 x 21 points. The numerical scheme featured a staggered grid (the "C" scheme of Arakawa and Mintz, 1974) with u, v and h on separate grids. The North and South boundaries were v-points with v set to 0, permanently. A centered difference time step equal to 10 min. was used, except once every 2 hours, when a Matsuno predictor-corrector step was used, to insure against separation into two computational modes.

The simulated "perfect" run was made from prescribed initial fields of h, u, and v, where h varied sinusoidally, while u and v were balanced geostrophically. The equations were integrated for 240 hours (10 days) and the fields stored every 2 hours. This run (heretofore referred to as "nature") was used as the verification for all other runs. The initial distribution of h and the resultant 6-hour field are shown in Figure 1.

The "error" runs were designed to test the relative magnitude and error growth patterns associated with each type of error. The first of these was the "initial" error including all effects of wrongly prescribing the initial field. Many of the simulation experiments mentioned previously chose to perturb the initial field by the addition of random errors. But many of the errors prevalent in the objective analysis of the numerical prediction models are not necessarily random, as mentioned earlier. The lack of data over wide expanses of the globe and the interpolation and assimilation of rare bits of information over large domains can easily be a more serious source of error than random instrument or human error. For this reason, both types of initial error were tested separately here. The first type was generated by adding random errors to h, u, and v and allowing the model to predict forward without further disturbance. This run will be designated as RE. The second (called DG for "data gap"), was generated by omitting information from the center of the field and extrapolating linearly from the surrounding points. Figs. 2 and 3 show the height contours at initial time and at 6 hours for RE and DG, respectively. These should be compared to Fig. 1 to assess the degree of departure from nature. Note that the initial field for RE is badly mottled, but some recovery is noted by 6 hours. DG has an apparent "hole" in the middle of the initial field which seems to cause a distortion in the field at 6 hours.

The second type of error investigated was physical error, which can be simulated in numerous ways. In the real world, it is difficult, if not impossible to evaluate the true physical error associated with incorrect physical assumptions or mathematical parameterization. In cases where these can be tested, results are usually too select to be meaningful. Williamson and Kasahara (1971) have attempted to show the effect of physical error in relation to initial error by demonstrating the effect of changing their boundary layer parameterization. But not all types of physical error behave in the same way. Obviously a "dry" model does not produce the same forecast as one which includes the effects of water vapor. In this experiment, we tested two types of physical error. One involved linearizing the right-hand side of (1)c by substituting an average value of H for h. The other resulted from the inclusion of a heating term added to (1)c which effectively raised h in the lower part of the field and decreased it in the upper part. The initial fields were the same as nature in both cases. The six hour h-field is shown in Fig. 4 for the linearized case (dubbed PE) and is not much different from nature; contours for the heated case are not available.

The third type of error is a simple truncation error produced by decreasing the grid resolution from a 42 x 21 network to 14 x 7 and increasing the grid spacing threefold. The new "error" will thus represent a mathematical truncation relative to the fine resolution. No physical changes were made in the model to compensate for the change in resolution and even the time step was not increased, although linear stability considerations would have allowed for it. The h contours for 0 and 6 hours are shown in Fig. 5 for the low resolution (LR) run. Note that initially there is considerable smoothing of the waves, with some of the closed contours appearing in nature missing in LR. At 6 hours, the gradients resemble more the initial conditions than the 6-hour nature field, with the tight gradients still occupying the northern portion of the domain rather than moving down to the southern portion as found in nature.

III. ERROR GROWTH PATTERNS

All the error runs continued until 240 hours and the root mean square (rms) error for the entire field was computed every 2 hours until 12 hours and every 6 hours thereafter. A plot of h-rms vs. time is presented in Fig. 6 and u-rms in Fig. 7 for PE, the heated case, LR, RE, and DG. They are obviously all quite different.

The physical errors show a considerable range of possibilities. The PE run asymptotes at fairly moderate levels. After a rapid rise during the first 6 hours, the error growth rate declines until it begins to oscillate at about 24 to 36 hours. Apparently the differences between the fields tend to remain small but some waves may be slightly out of phase. The heated case, on the other hand, shows a continued growth of error for the entire 10 days, probably because the magnitudes of the fields are considerably different in the heated case.

The LR case shows an almost predictable error growth pattern. There is an initial spurt of error growth followed by a choppy oscillation about some mean quantity. The oscillations are probably due to phasing differences caused by the differences in resolution between nature and LR. In linear wave equations, the truncation errors are also expected to oscillate since they are proportional to some order derivative of the time solution which consists of sinusoidal waves.

The initial errors present the most intriguing growth patterns in this study. RE shows a drop in error levels from the initial time until some asymptote is reached. The u-rms first increases as it adjusts to the error in h, but drops along with h immediately afterwards. DG, however, seems to maintain the same error level with a possible increase towards the end of the period.

One can understand the behavior of the initial errors from a discussion by Smagorinsky, et al., (1970) who blame the growth of initial error on baroclinic instabilities that amplify the initial perturbations until the perturbed field resembles the original field only as would a random climatalogical state . At the outset, the field goes through an adjustment period, according to Smagorinsky, et al., (1970), when the errors actually dip before rising. This dip was also mentioned by Halberstam (1974) and Blumen (1976a) using the barotropic equations. This study seems to indicate that the "adjustment" is a phenomenon associated only with random initial error. Other modes of error, similar to DG described here, may lead to different growth patterns where the noted dip does not occur. Apparently the dip is associated with the filtering of high-frequency waves by the numerical model. The noisy waves are a non-meteorological component which contaminate the field, and when they are removed by the smoothing and physics of the model, the field is brought into better agreement with other model fields or, at times, even with nature.

The decrease of error with time in RE seems to support Smagorinsky's, et al., (1970) contention that the baroclinic instabilities are responsible for error growth. In our study, a barotropic model was used, so that the initial errors either decrease or remain fairly constant. One must explain, however, why Miyakoda and Talagrand (1971) or Blumen (1976a) do show error growth even with barotropic models. They all insist that the non-linearity of the model is necessary for error growth, but it should not be a sufficient condition. In Miyakoda and Talagrand's (1971) study, a barotropic instability may have been created by proper boundary conditions producing sufficient wind shear. Blumen's model separates the geostrophic from the ageostrophic components of the vorticity and his analysis shows that the expected value of the rms error, assuming a random initial distribution, reaches an asymptotic value after a number of days, similar to realistic tests done with the National Center of Atmospheric Research (NCAR) model. His approach is quite different from a straighforward numerical approximation to the primitive equations or the vorticity form. His equations are, in effect, linear, with non-linear components added to them. This may have had an effect on the rate of computed error growth, although parallels to the primitive equations calculations should still exist.

Morel, et al., (1971) also used the barotropic case to study the effect of data assimilation on the rate of error growth. The initial conditions are also perturbed by random errors and simulated satellite data assimilated during an iterated forecasting-hindcasting cycle. The error is seen to decline during the assimilation cycle, but the control case (without the assimilation of data) is omitted. The reader is led to believe that the decrease in error is strictly due to the assimilation of data, rather than to the adjustment process. In light of the present study, their work may have to be reviewed with a non-assimilated run presented in comparison. If the assimilations are not totally responsible for the reduction of errors, then the recommended, expensive iterative process may not be worthwhile, especially with large numerical atmospheric models.

IV. SUMMARY AND CONCLUSIONS

A primitive equations barotropic model of the atmosphere has been used to test the effects of certain errors on numerical forecasts. The three types of errors investigated were physical errors, truncation errors, and initial errors. The physical errors consisted of a change in the model equations by 1. substituting a constant average value of H for the variable h in the divergent term of 1 (c) and 2. including a heating term which causes h to rise in the southern portion and decrease in the northern portion. The truncation error was generated by reducing the resolution to 1/3 of the original 42 x 21 grids. The initial errors were divided into a 1. random error and 2. sampling and interpolation error created by omitting the center of the field and filling the gap by interpolation.

Results show that physical errors have a large range, depending on the type of physics involved. Resolution errors grow initially and then oscillate about some mean quantity. Initial errors do not grow in this barotropic model. Instead, the random errors decrease until some asymptote is reached, while the interpolation error maintains a small oscillation about some mean value determined at the outset.

Indications are that physical errors are difficult to assess and probably more difficult to correct. The ones that are due to incorrect representation of the phenomena are the product of either unknown physics or unavoidable parameterization due to computer considerations. Truncation errors will always exist as long as finite differences are employed. Miyakoda, et al., (1971) have clearly shown that there is a critical resolution which must be surpassed in order for the forecast to be meteorologically meaningful. Beyond that, very little incremental benefit is achieved by increasing the resolution, at least for the short-term.

Most efforts in improving observations, such as the launching of satellites, are geared toward reducing the initial errors. This study observes that not all initial errors behave in the same way, and that they will not grow in the absence of instabilities. Simulation studies that make use of only random initial errors, may not be doing justice to the problem of initialization, since random errors are generally filtered out by the models themselves. On the other hand, areas and seasons of low baroclinicity may not require concentrated improvement of initial fields to improve forecasts.

Further investigations are planned to study the nature of error growth, especially with regards to initial error. Experiments performed at the Goddard Institute for Space Studies (GISS) with a realistic initial field are currently being documented by Cane, et al., (1977). A two-level baroclinic model is being developed at JPL to test the effects of baroclinicity on error growth, and whether areas of potentially serious errors can be predicted.

REFERENCES

Arakawa, A. and Y. Mintz, 1974: Notes for Workshop on UCLA General Circulation Model, Dept. of Meteorology, University of California at Los Angeles, Los Angeles, Calif.

Bengtsson, L., 1975: Four-dimensional assimilation of meteorological observations, GARP Publ. Series, No. 15, WMO-ICSU, Joint Organizing Committee, 76 pp. World Meteorological Organization, Geneva, Switzerland.

Blumen, W., 1976a: Experiments in atmospheric predictability: Part I. Initialization, J. Atmos. Sci., 33, 161-169.

____________, 1976b: Experiments in atmospheric predictability: Part II Data assimilation, J. Atmos Sci, 33, 170-175.

Cane, M., V. Cardone, I. Halberstam, M. Halem, and J. Ulrich 1977: Realistic simulation of a global observing system with application to Seasat-A marine wind data, (in preparation): preprints available from Department of Meteorology, Massachusetts Institute of Technology, Cambridge, Mass.

Halberstam, I., 1974: A study of three finite-difference schemes and their role in asynoptic meteorological data assimilation, J. Atmos. Sci., 31, 1964-1973.

Kasahara, A., 1972: Simulation experiments for meteorological observing systems for GARP, Bull. Amer Meteor Sci., 53, 252-264.

Miyakoda, K. and O. Talagrand, 1971: Assimilation of past data in dynamical analysis I, Tellus, 23, 310-317.

Morel, P., G. Lefevre, and G. Rabreau, 1971: On initialization and non-synoptic data assimilation, Tellus, 23, 197-206.

Smagorinsky, J., K. Miyakoda, and R.F. Strickler, 1970: The relative importance of variables in initial conditions for dynamical weather conditions, Tellus, 22, 141-157.

Williamson, D. and A. Kasahara, 1971: Adaptation of meteorological variables forced by updating, J. Atmos. Sci., 28, 1313-1324.

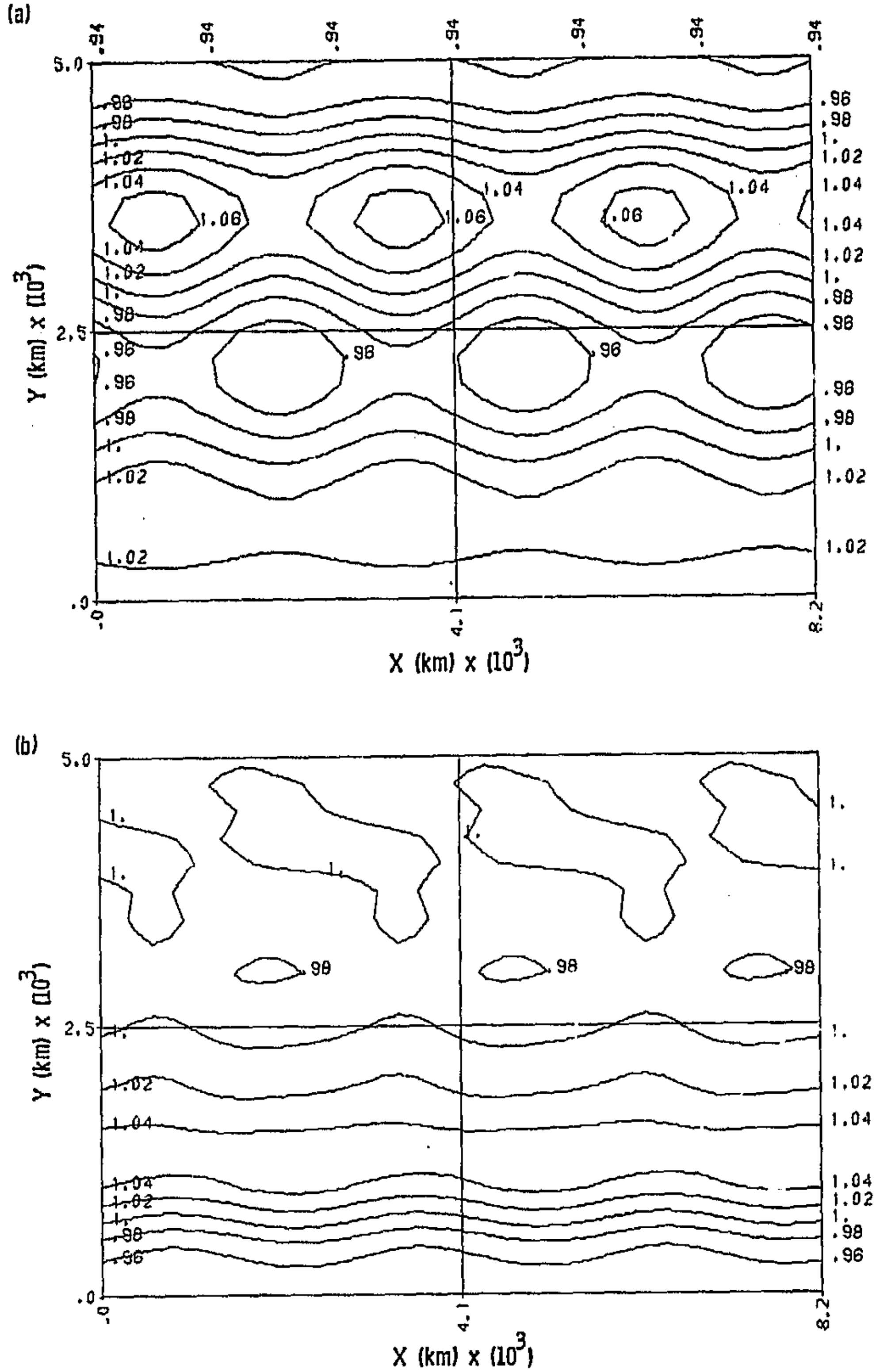

Fig. 1. Contours of h for the nature run at (a) 0 hours and (b) 6 hours (contour interval, 20 m)

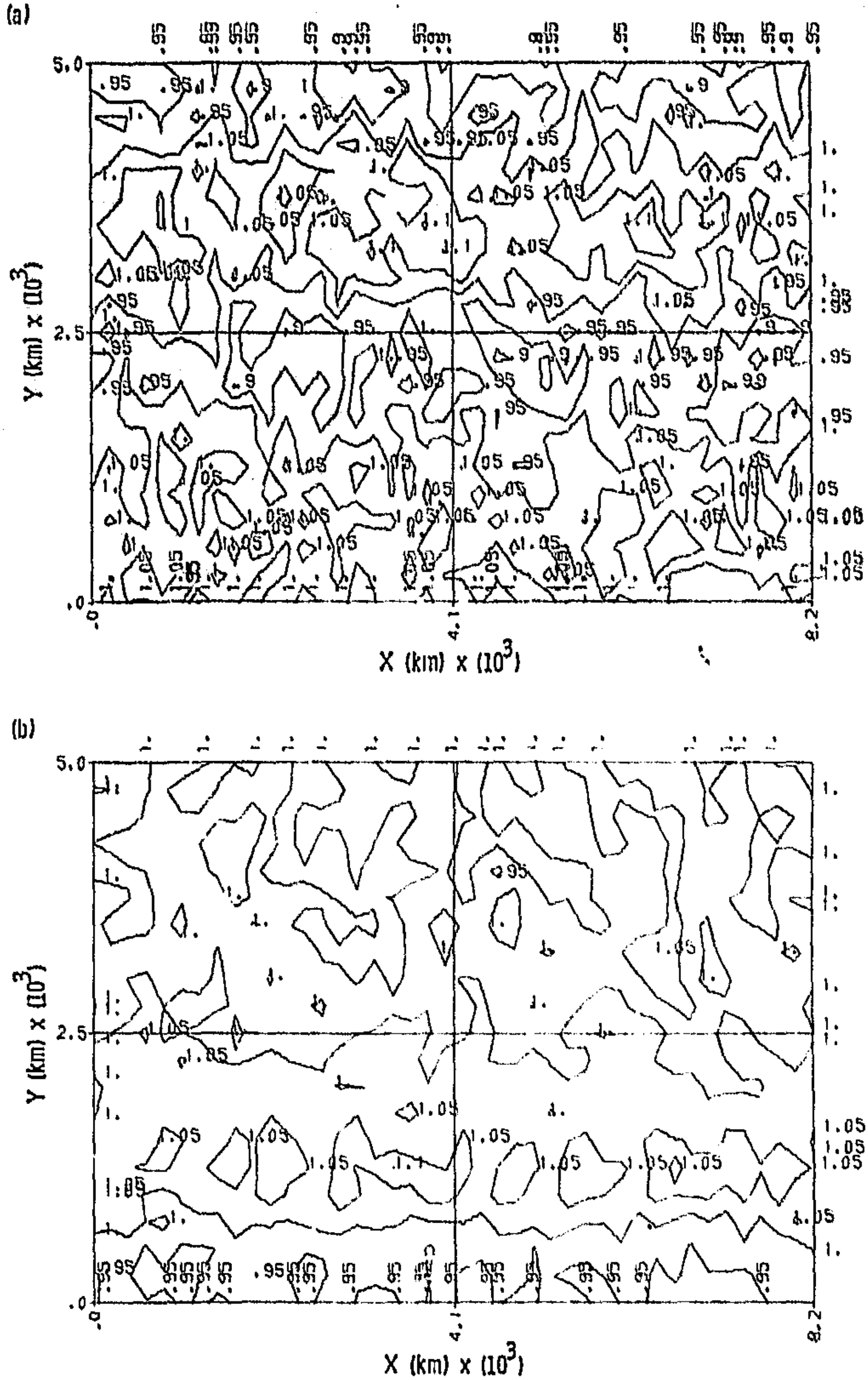

Fig. 2. Contours of h for RE at (a) 0 hours and (b) 6 hours

(a)

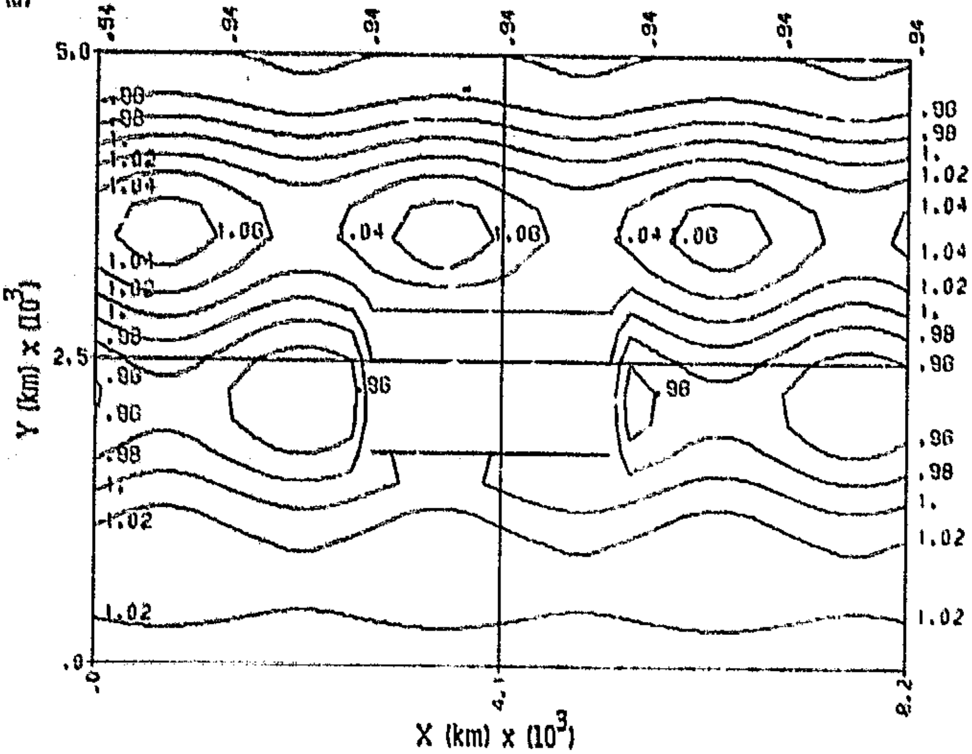

(b)

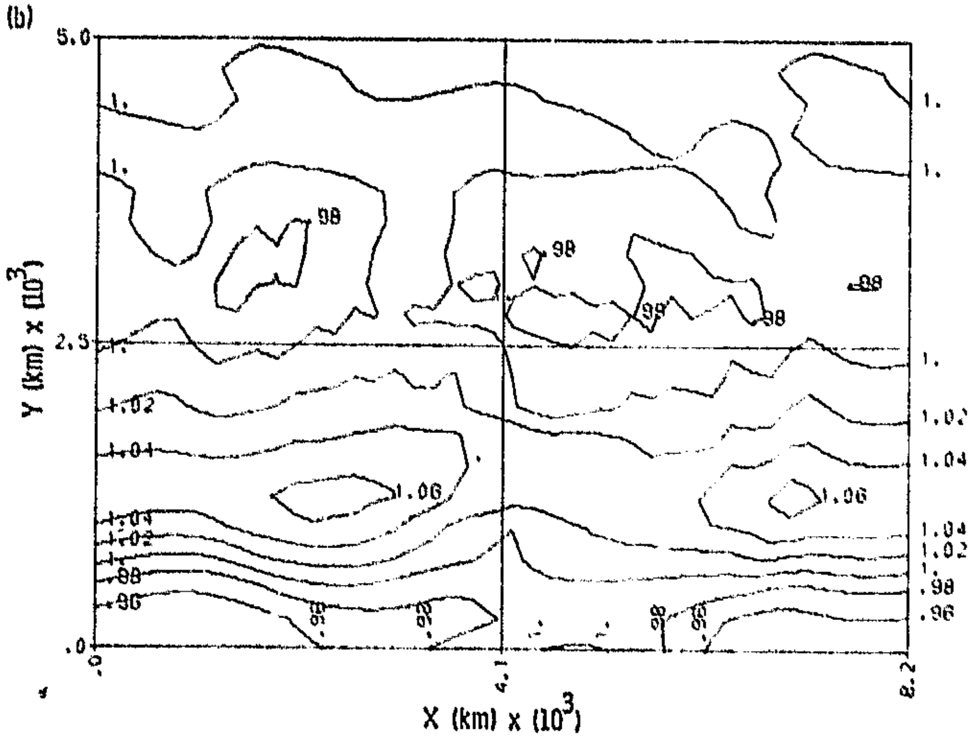

Fig. 3. Contours of h for DG at (a) 0 hours and (b) 6 hours

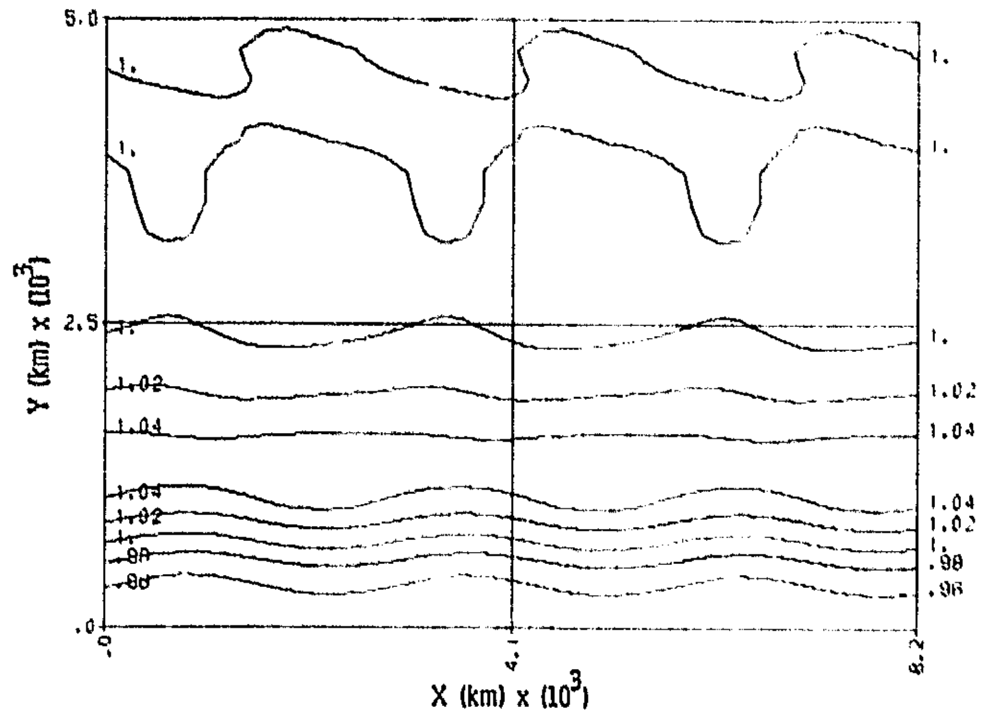

Fig. 4. Contours of h for PE at 6 hours

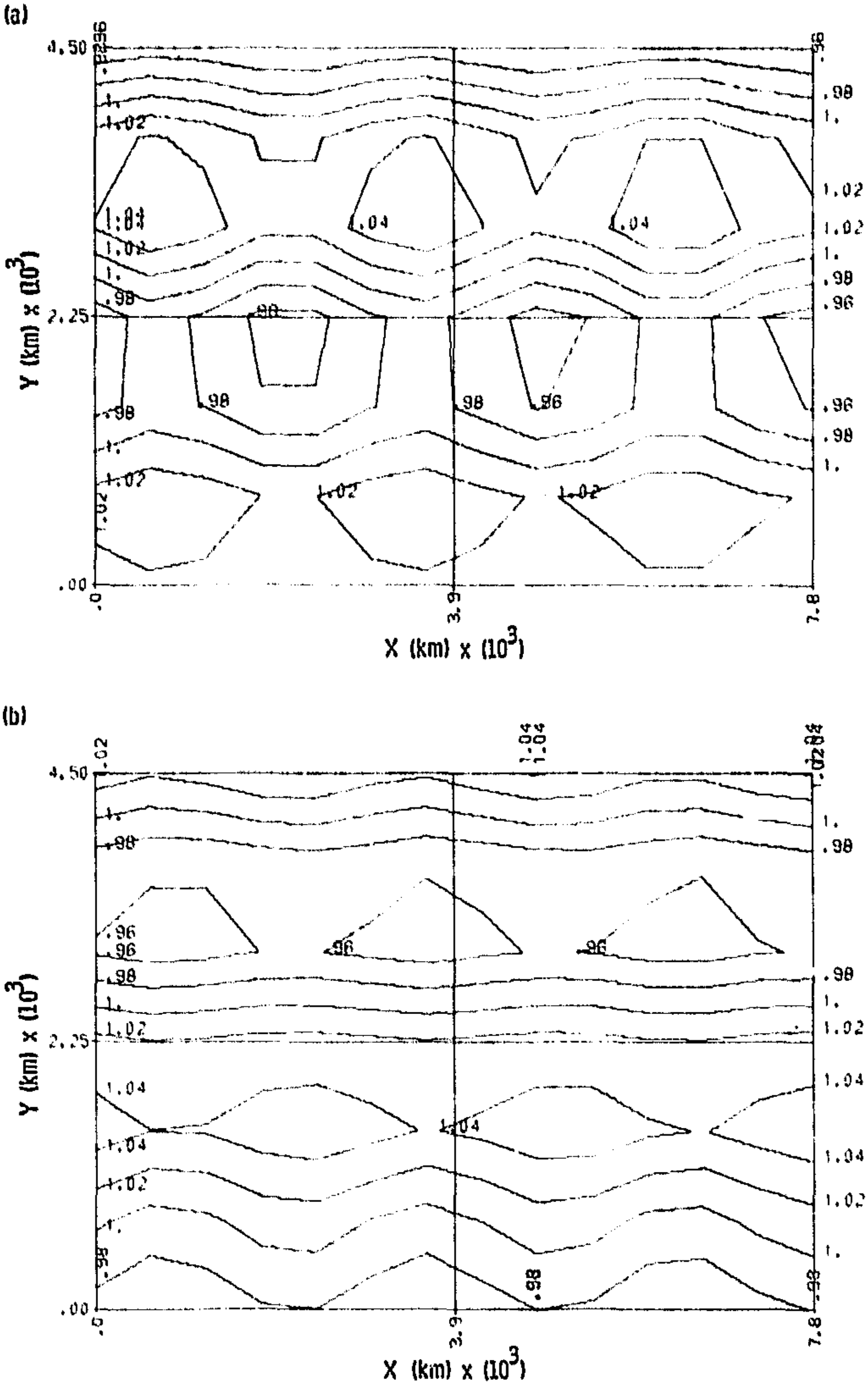

Fig. 5. Contours of h for LR at (a) 0 hours and (b) 6 hours

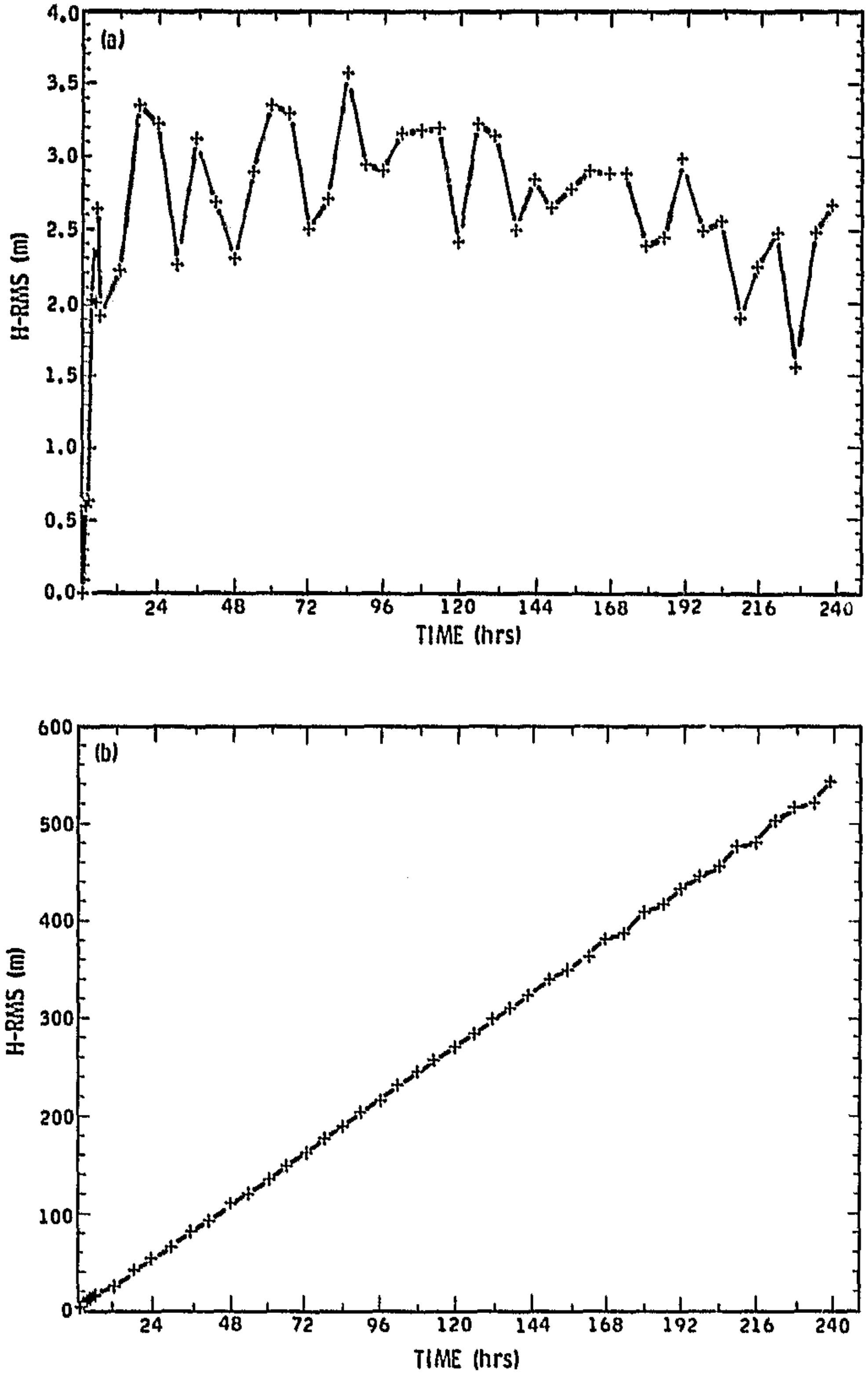

Fig. 6. Rms height errors vs time between the nature field and (a) PE, (b) the heated case, (c) LR, (d) RE, and (e) DG

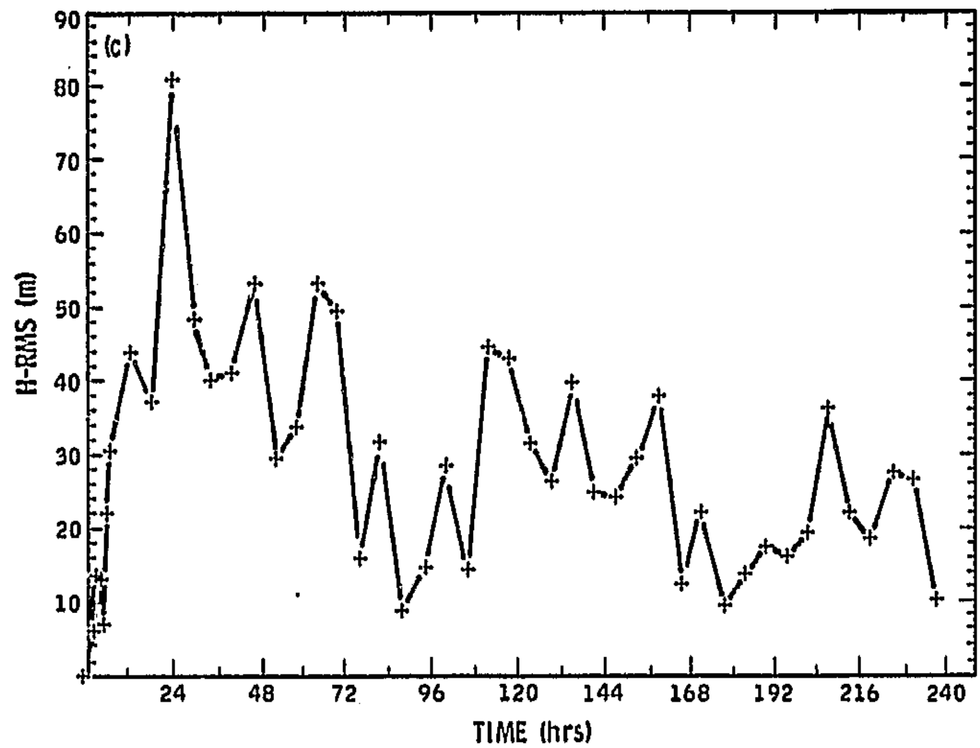
(c)
H-RMS (m)
90
80
70
60
50
40
30
20
10
24
48
72
96
120
144
168
192
216
240
TIME (hrs)

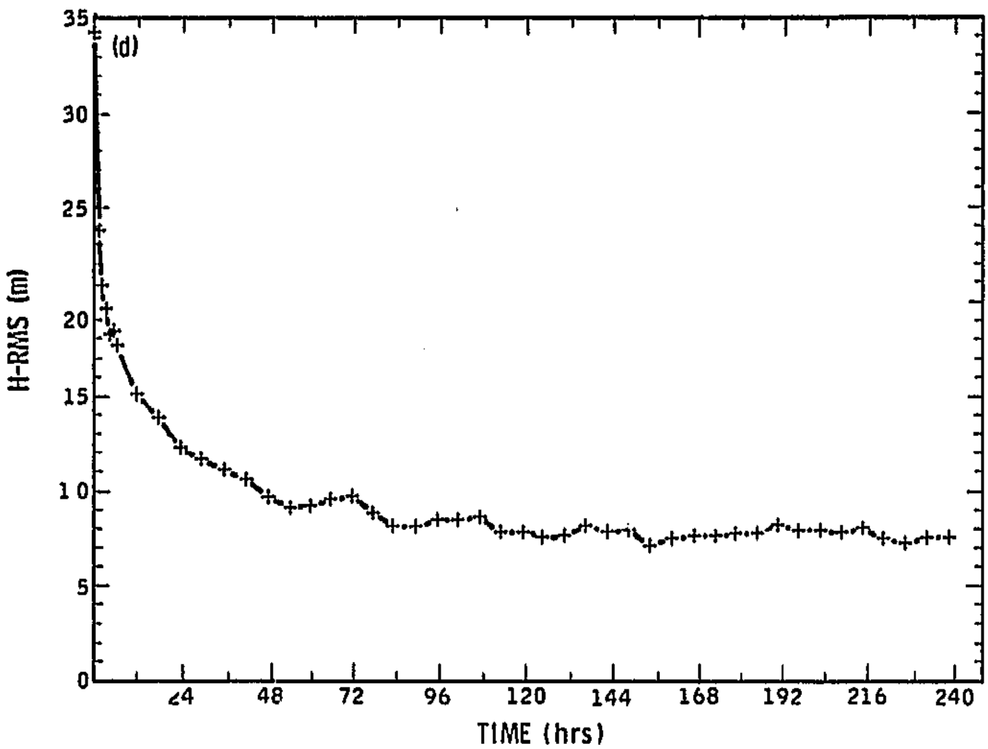
(d)
H-RMS (m)
35
30
25
20
15
10
5
0
24
48
72
96
120
144
168
192
216
240
TIME (hrs)

Fig. 6 (contd)

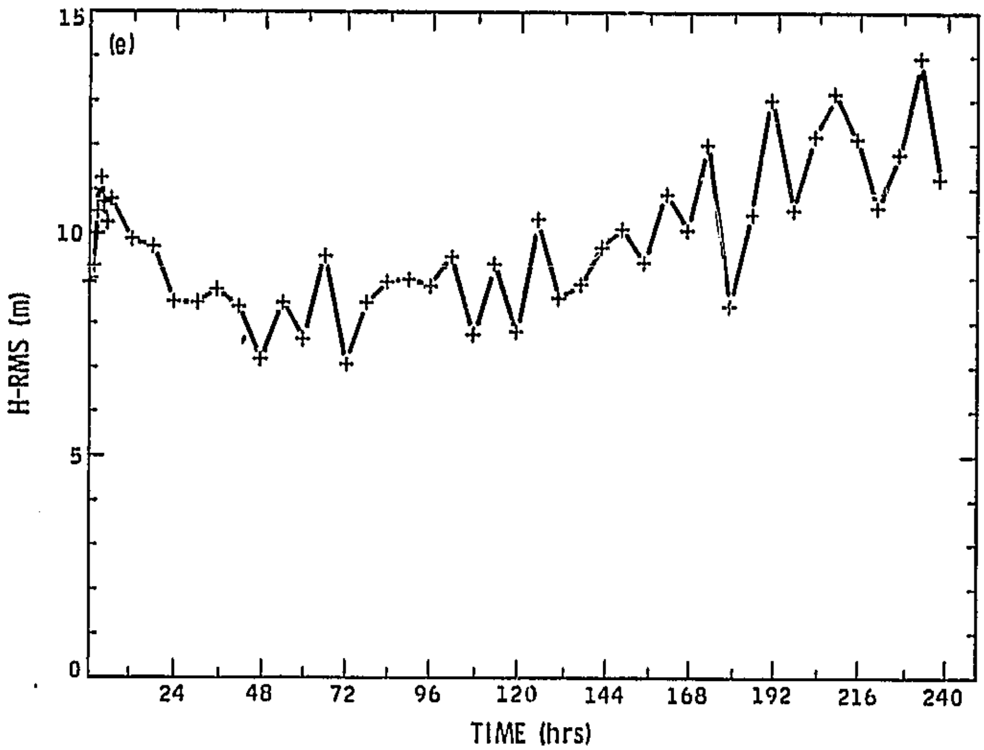

Fig. 6 (contd)

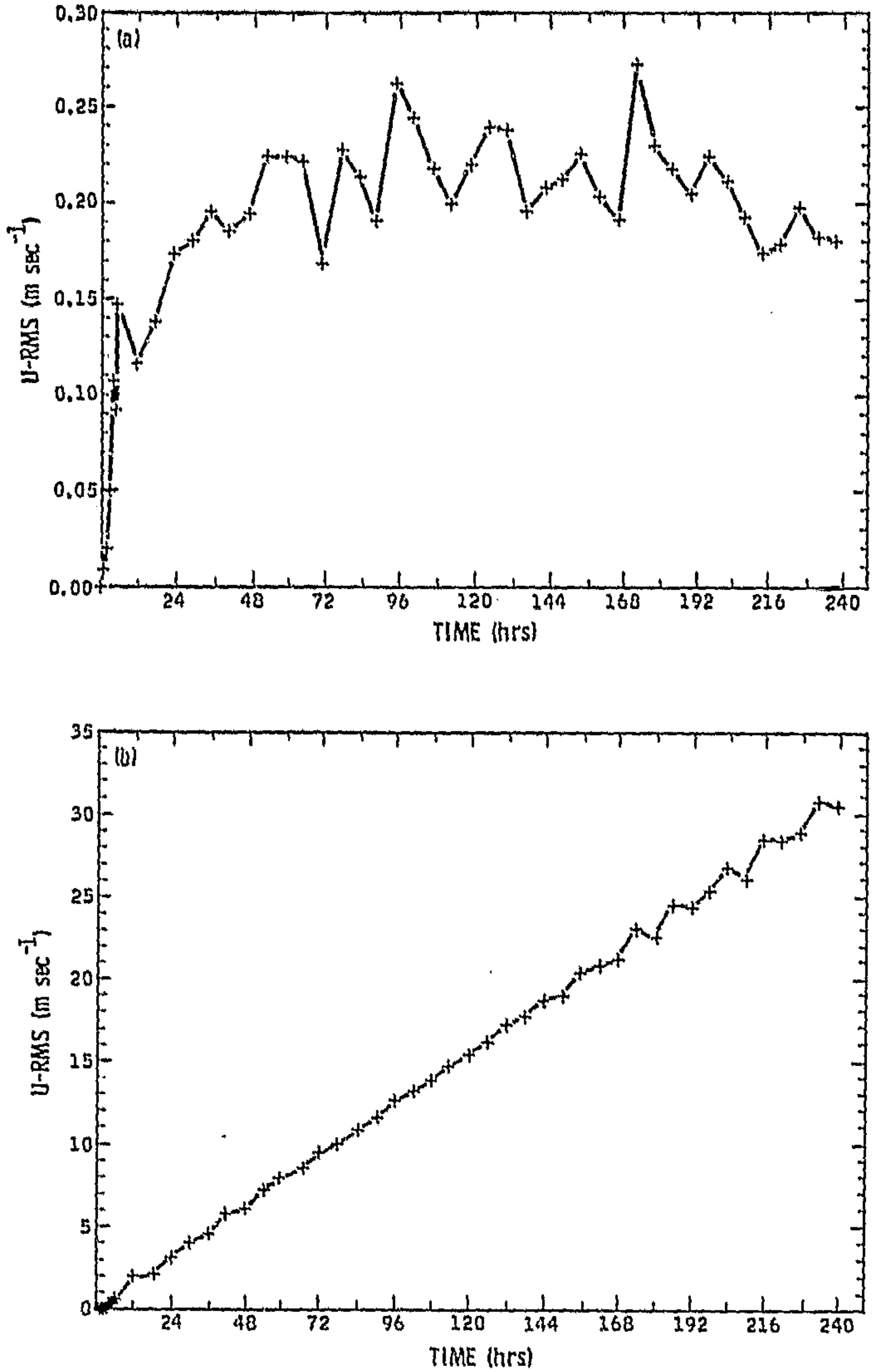

Fig. 7. Rms of u vs time between the nature field and (a) PE, (b) the heated case, (c) LR, (d) RE, and (e) DG

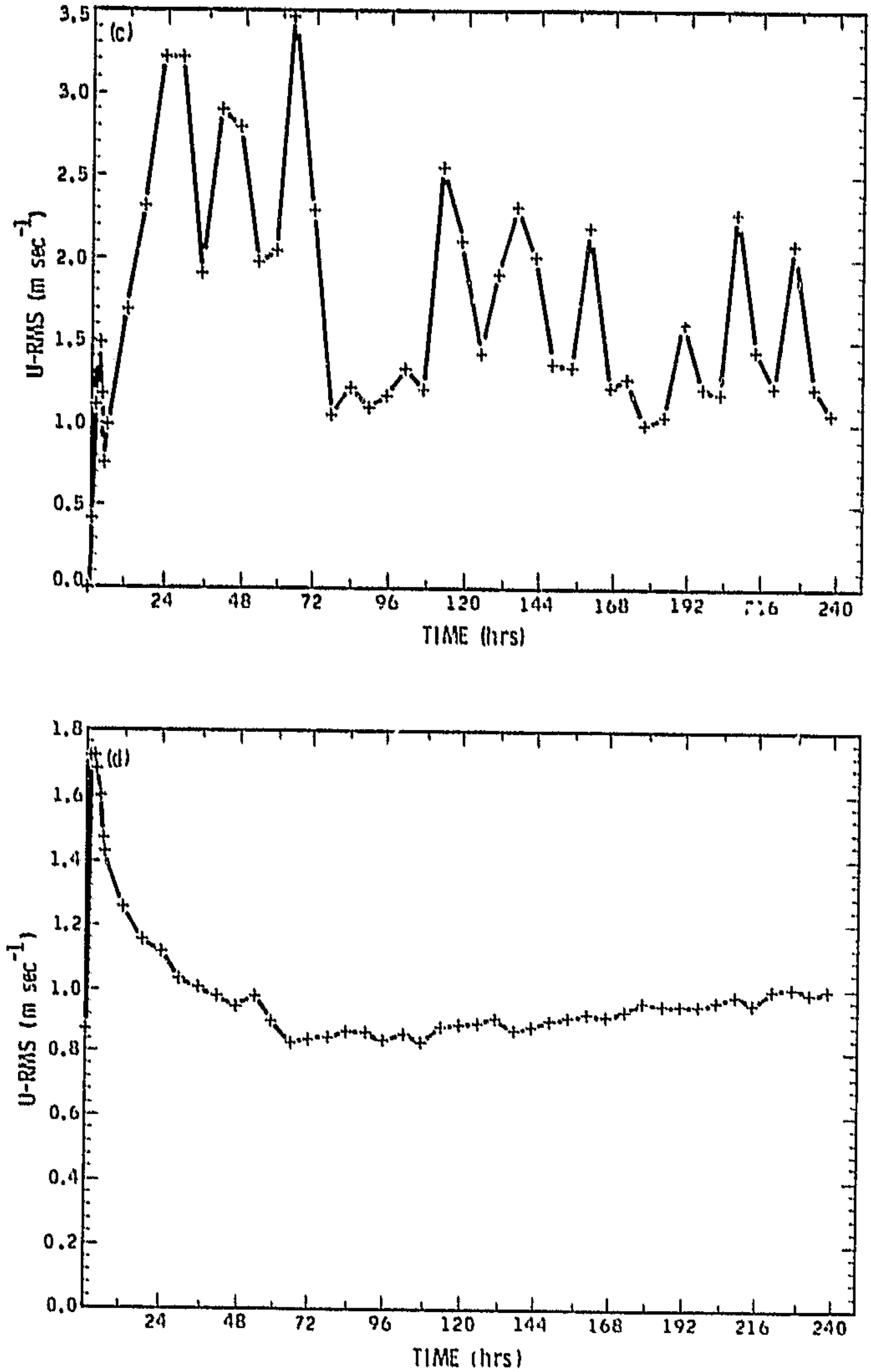
(c)
3.5
3.0
2.5
2.0
1.5
1.0
0.5
0.0
U-RMS (m sec^{-1})
24
48
72
96
120
144
168
192
240
TIME (hrs)
(d)
1.8
1.6
1.4
1.2
1.0
0.8
0.6
0.4
0.2
0.0
U-RMS (m sec^{-1})
24
48
72
96
120
144
168
192
216
240
TIME (hrs)

Fig. 7 (contd)

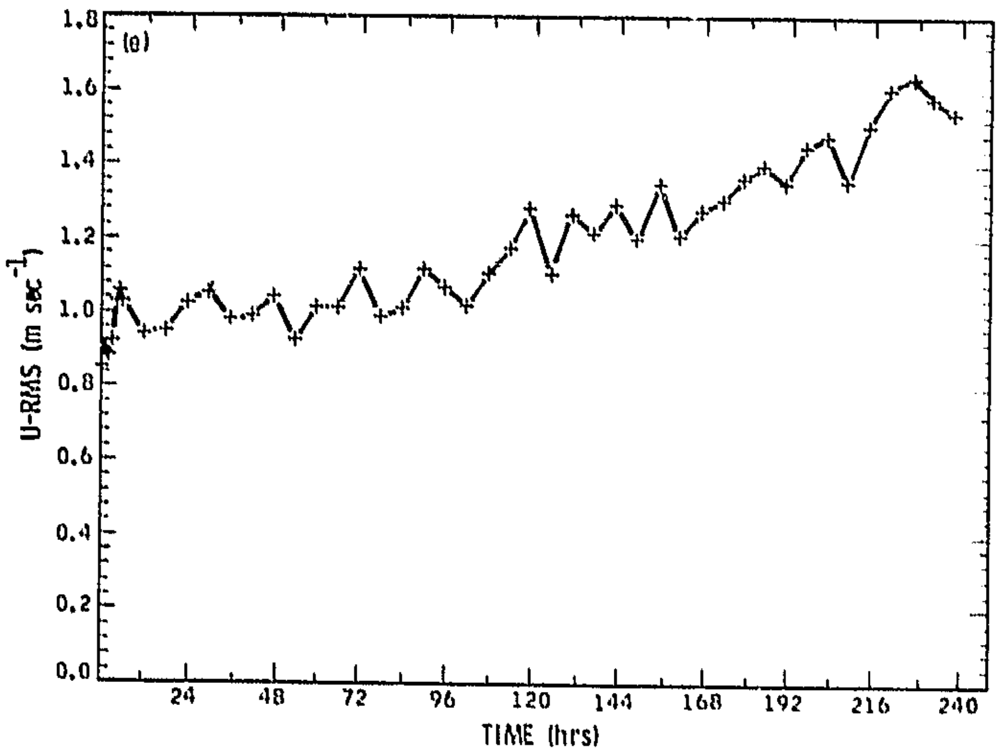
(e)
1.8
1.6
1.4
1.2
1.0
0.8
0.6
0.4
0.2
0.0
U-RMS (m sec^{-1})
24
48
72
96
120
144
168
192
216
240
TIME (hrs)

Fig. 7 (contd)